Journal of Geomatics Vol 8 No. 2 October 2014

Towards the expansion of orthometric correction in spherical harmonics

Raaed Mohamed Kamel Hassouna
Department of Civil Engineering, Faculty of Engineering in Shebin El-Kom, Minoufiya University
Shebin El-Kom, Minoufiya, Postal Code: 32511, Egypt
Email: rd3165@yahoo.com

(Received: May 09, 2013; in final form: Jul 08, 2014)

Abstract: In the current study, a proposed computational algorithm was attempted, in which the orthometric correction could be expanded in spherical harmonic series. Such harmonic synthesis algorithm utilized the unitless coefficients of geopotential models as scaled by the measured elevations or elevation differences. Comparisons were held with the orthometric corrections computed for some suggested leveling routes with observed gravity and elevation data in Egypt. The obtained results revealed the applicability of the proposed computational scheme. The orthometric correction values were explored over a square geographical window with very rough topography. Such window had a geographical extent of 12 arc-minutes, in both the latitude and longitude directions. In this respect, the respective SRTM3 elevations were used. The proposed algorithm proved to work well in spherical approximation. Based on the obtained results, it is recommended to apply the proposed algorithm for the computation of orthometric corrections.

Keywords: Orthometric correction, Spherical harmonics, Orthometric height, Geoid

1. Introduction

The orthometric height (OH) is the space curved distance from the geoid to the point of interest on the Earth's topographic surface. It can be computed from the geopotential number of a point and the mean value of gravity along the plumbline within the topography (i.e. between the geoid and the Earth's surface) (Heiskanen and Moritz, 1967). In this respect, various recent researches were introduced in order to rigorously compute such mean gravity value (Tenzer et al., 2005; Santos et al., 2006).

Synonymously, geometric leveling will yield a height difference between benchmarks, which requires an orthometric correction (OC) to end up with the target OH difference. Such OC could also be computed, based on the observed gravity values along leveling routes. Applying the OCs improves the accuracy and precision of leveling networks (Hwang and Hsiao, 2003). Because of their physical definition, OHs or OH differences have a wide range of practical and engineering applications (Ellmann et al., 2007).

Recent geopotential missions are continuously refining high resolution satellite-only products. The determination of OH was sought via satellite-only models' derived geopotential numbers and analytical models for both the gravity vector and plumbline curvature at the point of interest. This approach has been accomplished without any explicit information about the topographic mass distribution (Manoussakis et al., 2009). Also, previous studies investigated the use of the high-degree model EGM2008 (Pavlis et al., 2008) for the derivation of gravity at the locations of benchmarks, in order to derive the OCs for different leveling lines. In this respect, it was suggested that EGM2008-based gravity could be a reasonable representation of the gravity field for computing gravity-based height corrections (Filmer et al., 2010). Compared with EGM2008, lower degree geopotential models (of degree and order 360) also showed a great capability to densify or replace observed gravity along suggested leveling routes for orthometric correction assessment (Hassouna, 2013).

The objective of the current study is to propose and try a computational algorithm, which expands the OC in spherical harmonic series, based on geopotential harmonic coefficients and elevation data. In this respect, three recent geoptential harmonic models are used. This is accompanied with comparisons to the results obtained for some suggested leveling lines with observed gravity data in Egypt. Also, based on the proposed algorithm, the OC behaviour is investigated over a 12x12 arc-minute geographical widow with very rugged topographic features. For this purpose, the 3x3 arc-second SRTM3 elevation model is used (USGS, 2006). Finally, the effect of spherical approximation on the proposed algorithm is studied.

2. Basics of the proposed algorithm

Based on a geopotential harmonic model, the constant geopotential, W_0, on the geoidal surface may be expressed at a certain point as follows (Heiskanen and Moritz, 1967)

$$W_0 = \frac{GM}{r}\sum_{n=0}^{L}\sum_{m=0}^{n}\left(\frac{a}{r}\right)^n\left[(\overline{C}_{nm}\cos m\lambda + \overline{S}_{nm}\sin m\lambda)\,\overline{P}_{nm}(\cos\theta)\right] + \frac{1}{2}\omega^2(X^2+Y^2), \quad (1)$$

with

L the maximal degree of the geopotential harmonic model,

GM the universal gravitational constant,
a the equatorial radius,
λ the geodetic longitude,
θ the geocentric co-latitude,
r the geocentric radius till the ellipsoidal point,
$\overline{C}_{nm}$ the fully normalized spherical harmonic C-coefficients of degree n and order m,
$\overline{S}_{nm}$ the fully normalized spherical harmonic S-coefficients of degree n and order m,
$\overline{P}_{nm}(\cos\theta)$ the fully normalized associated Legendre function of degree n and order m,
X &Y the geocentric Cartesian coordinates of the ellipsoidal point,
ω the mean angular speed of the Earth (ω = 7.292115x10^{-5} radian/second).

Based on Eq. (1) and neglecting the small angle between the geocentric radius and the direction of the vertical, the geocentric radius, R_0, of the geoid may be expressed at the point under consideration as follows (Burša, 1975; Santos et al., 2006; Kotsakis et al., 2012)

$$R_0 = r\sum_{n=0}^{L}\sum_{m=0}^{n}\left(\frac{a}{r}\right)^n\left[(\overline{C}_{nm}\cos m\lambda + \overline{S}_{nm}\sin m\lambda)\,\overline{P}_{nm}(\cos\theta)\;\right] + \frac{1}{2}\omega^2\frac{(X^2+Y^2)}{\gamma}, \tag{2}$$

where γ is the normal gravity induced by the reference ellipsoid, which may be expressed by (Moritz, 1980)

$$\gamma = \gamma_e\frac{\left(1+k\sin^2\varphi\right)}{\sqrt{1-e^2\sin^2\varphi}}, \tag{3}$$

with
e the first eccentricity of the ellipsoid,
φ the geodetic latitude,
γ_e the equatorial normal gravity on the ellipsoid,

$$k = \left(\frac{b\gamma_p}{a\gamma_e} - 1\right), \tag{4}$$

b and γ_p being the semi-minor axis and polar normal gravity, respectively (Moritz, 1980).

Similarly, and as can be inferred from Burša (1971) and Santos et al. (2006), the geocentric radius, R, of the level surface through the terrain point may be expressed as

$$R = r_t\sum_{n=0}^{L}\sum_{m=0}^{n}\left(\frac{a}{r_t}\right)^n\left[(\overline{C}_{nm}\cos m\lambda + \overline{S}_{nm}\sin m\lambda)\,\overline{P}_{nm}(\cos\theta)\;\right] + \frac{1}{2}\omega^2\frac{(X_t^2+Y_t^2)}{\gamma}, \tag{5}$$

where
r_t the geocentric radius till the relevant telluroidal point (on the sphero-potential surface),
X_t &Y_t the geocentric Cartesian coordinates of the telluroidal point.

Now, the OH of the terrain point could be expressed as follows (Ellmann et al., 2007)

$$OH = R - R_0. \tag{6a}$$

So, substituting for the harmonic parts of R_0 and R from Eqs. (2) and (5), respectively; approximating $(a/r_t)^n$ with $(a/r)^n$; and appropriately accounting for the rotational parts; Eq. (6a) yields

$$\begin{aligned} OH &\approx (r_t - r)\sum_{n=0}^{L}\sum_{m=0}^{n}\left(\frac{a}{r}\right)^n\left[(\overline{C}_{nm}\cos m\lambda + \overline{S}_{nm}\sin m\lambda)\,\overline{P}_{nm}(\cos\theta)\;\right] + \frac{1}{2}\omega^2\frac{(r_t-r)^2\sin^2\theta}{\gamma} \\ &= (r_t - r)\sum_{n=0}^{L}\sum_{m=0}^{n}\left(\frac{a}{r}\right)^n\left[(\overline{C}_{nm}\cos m\lambda + \overline{S}_{nm}\sin m\lambda)\,\overline{P}_{nm}(\cos\theta)\;\right] + \frac{1}{2}\omega^2\frac{\left[(X_t-X)^2+(Y_t-Y)^2\right]}{\gamma}, \end{aligned} \tag{6b}$$

in which the second (rotational) term has been rigorously derived by integrating the difference between the centrifugal accelerations at r_t and r. In the case of spherical approximation, which will be applied in Section 5, both a and r are taken equal to the mean radius of the Earth (Heiskanen and Moritz, 1967). Thus, while in spherical approximation differences at the km level might be ignored without significantly affecting the (a/r) ratio, the above approximation neglects differences that are equal to the elevations only. So, taking $(a/r_t)^n = (a/r)^n$ in Eq. (6b) sounds realistic and even more accurate than the spherical approximation itself.

Accordingly, Eq. (6b) could be further modified and reduced to

$$OH \approx H^* \left\{ 1 + \sum_{n=2}^{L} \sum_{m=0}^{n} \left(\frac{a}{r} \right)^n \left[(\overline{C}_{nm} \cos m\lambda + \overline{S}_{nm} \sin m\lambda) \overline{P}_{nm}(\cos\theta) \right] \right\} + \frac{1}{2} \omega^2 \frac{H^{*2} \sin^2 \theta}{\gamma}, \quad (6c)$$

where H^* is the normal height. The difference between the normal height and OH of the terrain point is given by (Heiskanen and Moritz, 1967)

$$H^* - OH = N - \zeta, \quad (7)$$

ζ and N being the height anomaly and geoidal height, respectively. In the extreme case, such difference, which is known to be correlated with topography, could amount to 3.62 m for Himalayas (Bagherbandi and Tenzer, 2013). An insight into Eq. (6c) reveals that compared to the numerical power of the harmonic coefficients and the small magnitude of ω^2, this difference could be safely ignored. Particularly, using a hypothetical extreme value of 3.62 m for $(H^* - OH)$ in the investigated region, which is much larger than the actual local values, the preliminary computations resulted in an OC error that is less than 1 mm. Consequently, the value of H^* may be simply replaced in Eq. (6c) by, say, the leveled elevation, H. Obviously, much smaller errors will be committed in the case of the OC of leveled height differences, which will be discussed in Section 3. In such case, the differences among the $(H^* - OH)$ values would be the items to be neglected.

So, substituting for H^* by H in Eq. (6c) and rearranging, the OC may be expressed as follows

$$OC = OH - H = H \sum_{n=2}^{L} \sum_{m=0}^{n} \left(\frac{a}{r} \right)^n \left[(\overline{C}_{nm} \cos m\lambda + \overline{S}_{nm} \sin m\lambda) \overline{P}_{nm}(\cos\theta) \right] + \frac{1}{2} \omega^2 \frac{H^2 \sin^2 \theta}{\gamma}. \quad (8)$$

The first (harmonic) term in Eq. (8) is obviously the dominant part of the OC, whereas the second term (or the rotational constitute) of the OC is small. In particular, the subsequent computations of the latter term will show an extreme value that is negligible (about 0.5 mm). However, for higher elevations with smaller latitudes, such term could be significant.

Equation (8) implies that the harmonic part of the OCs of the elevations could be looked upon as resulting from the modulation of the topographic signal (or elevations) on the gravitational signal, as expressed by the (unitless) geopotential harmonic coefficients, beginning with degree two. On the other hand, the small rotational contribution could represent the inherent relative repulsions between the level surfaces and the geoid.

3. Generalizing the algorithm to leveled height differences

Considering two benchmarks A and B, the geocentric radii of the relevant level surfaces may be computed from Eq. (5). So, a similar version of Eq. (8) may be derived to express the OC_{AB}, relevant to the geometrically leveled height difference, ΔH_{AB}, as follows

$$OC_{AB} = \Delta OH_{AB} - \Delta H_{AB} = \Delta H_{AB} \sum_{n=2}^{L} \sum_{m=0}^{n} \left(\frac{a}{r_A} \right)^n \left[(\overline{C}_{nm} \cos m\lambda_B + \overline{S}_{nm} \sin m\lambda_B) \overline{P}_{nm}(\cos\theta_B) \right] + \frac{1}{2} \omega^2 \frac{\Delta H_{AB}^2 \sin^2 \theta_B}{\gamma_B}, \quad (9)$$

where

- ΔOH_{AB} the orthometric height difference, measured along the pumbline of the end benchmark B, from the level surface of A to B,
- θ_B & λ_B the geocentric co-latitude and geodetic longitude, respectively, of the end benchmark B,
- r_A the geocentric radius of the level surface through the start benchmark A, computed at the location of the end benchmark B,
- γ_B the normal gravity relevant to the end benchmark B (via Eq. 3).

Taking into account a certain spirit leveling route from benchmark A to benchmark B, Eq. (9) could be cumulatively applied to the relevant level set-ups, as follows

$$OC_{AB} = \Delta OH_{AB} - \Delta H_{AB} = \sum_{i=1}^{ns} \left\{ \delta h_i \sum_{n=2}^{L} \sum_{m=0}^{n} \left(\frac{a}{r} \right)^n \left[(\overline{C}_{nm} \cos m\lambda + \overline{S}_{nm} \sin m\lambda) \overline{P}_{nm}(\cos\theta) \right] + \frac{1}{2} \omega^2 \frac{\delta h_i^2 \sin^2 \theta}{\gamma} \right\}, \quad (10)$$

with

- ns the number of level set-ups,
- δh_i the leveled height increment at the i^{th} level set-up,

θ, λ and γ stand for the location of the fore-sight of the i[th] level set-up and the relevant normal gravity, respectively,

r the geocentric radius of the level surface through the back-sight point, computed at the fore-sight location.

In Eqs. (10) and (9), regarding the practically small magnitudes of δh_i or even ΔH_{AB}, the second (rotational) term would be very small and could be neglected (see Kotsakis et al., 2012).

In the current work, computer software was prepared to accomplish the proposed algorithm in Eq. (8), (9) or (10), based on an existing spherical harmonic synthesis code (Forsberg and Tscherning, 2008). The prepared software was efficient, in terms computer time.

Alternatively, according to Hwang and Hsiao (2003), the OC along a spirit leveling line, AB, may be rigorously expressed as

$$OC_{AB} = \frac{1}{\overline{g}_B}\sum_{i=1}^{ns}\left(g_i - \overline{g}_B\right)\delta n_i + \left(\frac{\overline{g}_A}{\overline{g}_B} - 1\right)H_A, \quad (11a)$$

g_i being the observed gravity relevant to the i[th] level set-up; and $\overline{g}_A$ and $\overline{g}_B$ are the mean gravity (in mgals) along the plumblines at A and B, respectively. Such mean gravities may be expressed as

$$\overline{g}_A = g_A + 0.0424H_A,$$
$$\overline{g}_B = g_B + 0.0424H_B, \quad (11b)$$

where g_A and g_B are the observed gravity values (in mgals) at A and B, respectively. Equation (11) will be used in Section 4 for the validation of the proposed algorithm, as represented by Eq. (8) to (10).

4. Algorithm validation and results

In order to validate the proposed algorithm, three suggested different leveling routes were considered. Table 1 lists a brief description of the geographical and topographic features of the three leveling courses. In particular, route (I) has a major south-north extension with moderate topographic variations. Course (II) is nearly west-east aligned, associated with almost flat topography. Finally, route (III) runs in a north-east direction and exhibits rough terrain variability. All the proposed routes possess observed gravity and elevation data, but are not parts of the Egyptian precise leveling network, whose details were not available.

Table 1: Geographical extension and topographic features of the validating leveling lines

Route	$\Delta\varphi$ (minutes)	$\Delta\lambda$ (minutes)	ΔH (m)
(I)	139.03	27.37	-24.680
(II)	0.17	0.88	-1.372
(III)	44.03	15.50	-58.510

Equation (11) was firstly used for computing relevant values of OCs, based on the observed gravity and elevation values along the three routes. Then, relevant OCs were independently computed, based on Eq. (10), utilizing the coefficients of three geopotential models and the observed elevation data. These models are GGM03C (Tapley et al., 2007), GOCO03S (Mayer-Gürr et al., 2012) and DGM-1S (Hashemi Farahani et al., 2012). Table 2 summarizes the constants of the three harmonic models.

Table 2: Elements of the three geopotential harmonic models

Model	L	GM ($m^3\ s^{-2}$)	Equatorial radius a (m)
GGM03C	360	$3.986004415 \times 10^{14}$	6378136.30
GOCO03S	250	$3.986004415 \times 10^{14}$	6378136.30
DGM-1S	250	$3.986004415 \times 10^{14}$	6378136.60

Furthermore, the OCs were calculated for the three routes, based on Eqs. (8) and (9). While Eq. (8) was used to assess the differences $(OC_B - OC_A)$, the role of Eq. (9) was to compute OC_{AB} directly, in terms of ΔH_{AB}. The purpose of such additional evaluations was to numerically check the proposed algorithm, regarding its numerical significance. In other words, one would check the algorithm in Eq. (10), which should use cumulative small height increments, regarding its ability to recover the OCs. During the evaluation of Eq. (8) to (10), the locations of all points were expressed relative the WGS-84 reference ellipsoid. Also, the three harmonic models have the same GM value. So, no relevant scaling was required in the evaluation of Eq. (8) to (10).

Firstly, Table 3 lists the statistics of the elevations pertaining to the three leveling routes, along with their OCs as computed at each point from DGM1-S by Eq. (8). It should be mentioned that, to the nearest two decimal places of 1 mm, the same values for the OCs resulted from the other two geopotential models. Obviously, the relative roughness of the terrain routes, in terms of the standard deviation of elevations, is reflected by the corresponding OCs values along with their standard deviations.

Table 3: Statistics of the elevations and *OCs* pertaining to the points of the three leveling routes (based on DGM-1S)

Line	Item	Mean	Standard deviation	Minimum	Maximum
I	H (m)	34.85	7.84	22.50	49.24
	OC (mm)	6.133	1.922	3.294	9.735
II	*H* (m)	186.04	0.448	185.371	186.852
	OC (mm)	51.744	0.127	51.551	51.969
III	*H* (m)	275.75	18.557	224.04	295.59
	OC (mm)	60.808	4.929	47.517	65.160

Table 4 illustrates the values of *OCs* , corresponding to the three routes, as computed by the above described procedures. An important remark is that the *OCs* , computed from Eq. (8) to (10), are practically invariant with respect to the maximum resolution of the used geopotential models.

Table 4: Comparison among the *OCs* values computed based on the terrestrial data and the proposed algorithm (units: mm)

Method	Harmonic model	*OC* (Line I)	*OC* (Line II)	*OC* (Line III)
Rigorous Eq. (11)	(N/A)	-7.058	0.149	-13.629
Proposed (Eq. 10)	GGM03C	-4.294	-0.381	-12.508
	GOCO03S	-4.294	-0.381	-12.507
	DGM-1S	-4.294	-0.381	-12.507
Proposed (Eq. 9)	GGM03C	-3.582	-0.381	-12.410
	GOCO03S	-3.582	-0.381	-12.407
	DGM-1S	-3.582	-0.381	-12.407
Proposed (Eq. 8)	GGM03C	-6.216	-0.390	-17.103
	GOCO03S	-6.214	-0.389	-17.124
	DGM-1S	-6.214	-0.389	-17.124

5. Exploring the *OC* values over an SRTM3 window

Equation (8) was used to explore the elevations *OCs* over a square geogpahical window bounded by (26.8° N ≤ φ ≤ 27° N; 33.2° E ≤ λ ≤ 33.4° E). Such domain is a part of the Egyptian East Desert and the Red Sea Mountains, and hence, is associated with a very rough topography. In this respect, the 3x3 arc-second elevations of the SRTM3 elevation model are used.

Such resolution corresponds to a nominal spacing of 90 m. Compared to ground surveyed elevations, the accuracy of such model in less rough terrain in Egypt is about of 3.50 m (Abdel-Gawad et al., 2010). In the sense of Section 2, such accuracy range would be sufficient for a relatively accurate *OC* computation by the proposed algorithm. Both the GGM03C and GOCO03S were used to evaluate the relevant *OCs* .

Table 5 summarizes the statistics of the elevations and *OCs* pertaining to the investigated SRTM3 window. Moreover, it shows the relevant values of the non-harmonic term in Eq. (8). Figures 1 and 2 show 3D surface maps for the SRTM3 elevations and the associated *OC* values based on GGM03C, respectively. Obviously, the two figures show the very high correlation among the elevations and their *OCs* .

In spherical approximation, the factor (a/r), in Eq. (8) to (10), would simply reduce to unity. Also, the geocentric latitude will be replaced by the geodetic latitude. Specifically, the effect of spherical approximation on the *OCs* , computed by Eq. (8), was investigated over the same rugged terrain window. Table 6 illustrates the statistics of the differences of the two sets of *OCs* (without and with spherical approximation), as computed based on GOCO03S. From Table (6), regarding the investigated region, these differences are negligible. This could imply that the proposed algorithm works well in spherical approximation.

Table 5: Statistics of the elevations and *OCs* for the SRTM window (based on GOCO-03S and GGM03C)

Item	Mean	Standard deviation	Minimum	Maximum
H (m)	769	186	466	1540
OC (mm) (GOCO-03S)	165.153	39.808	100.201	328.559
OC (mm) (GGM-03C)	165.181	39.818	100.213	328.627
2nd term (mm)	0.135	0.068	0.047	0.512

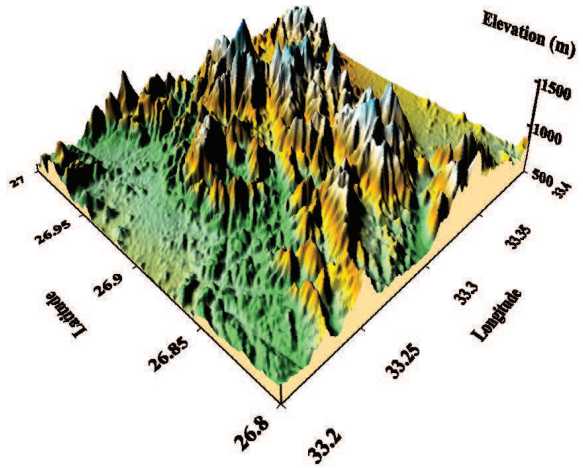

Figure 1: SRTM3 elevations over the selected window

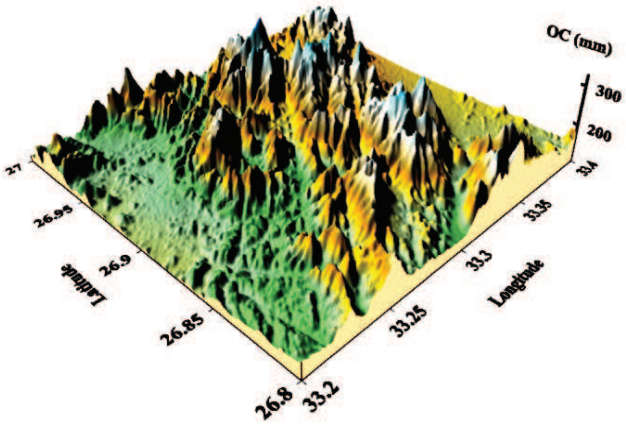

Figure 2: 3D map for the *OCs* over the SRTM3 window (based on GGM03C)

Table 6: Statistics of the differences between two sets of *OCs* for the SRTM window (without and with spherical approximation based on GOCO-03S)

Mean (mm)	Standard deviation (mm)	Minimum (mm)	Maximum (mm)
0.194	0.036	0.129	0.309

6. Conclusions

Regarding Table 4, the results of route (II) could imply the capability of the proposed algorithm (Eq. 8 to 10) to recover the (expected) small values of the *OCs* , for a west-east running leveling route over almost flat terrain. This in turn may imply an eventual reliability of the proposed algorithm.

For route (III), the *OCs* relevant to Eqs. (9) and (10) are close to the validating results of Eq. (11), with small differences. This could imply that numerically, the incremental procedure in Eq. (10) could have efficiently recovered the magnitudes of the*OCs* over rugged terrain. Also, such result may indicate that the differencing procedure, as represented by Eq. (9), could be a promising tool for recovering the *OCs* , without any need for intermediate information and/or treatment along such leveling lines. However, Eq. (8) seemed to fail in accurately recovering the *OCs* over such rough terrain. This leveling line might require detailed height difference information for the leveling route, as represented by Eq. (9) or Eq. (10). This result might be compatible with a thought that the *OC* value could be highly dependent on a leveling path over rough terrain.

Alternatively, only the results of Eq. (8) are close to those of Eq. (11) for route (I), with differences less than 1mm. This latter result could imply that accurate *OCs* may be obtained via Eq. (8) in moderately varying terrain, for which the main features of terrain suffice. However, Eqs. (9) and (10) could have exhibited a loss in numerical significance during the assessment of *OCs* , as a consequence of the associated differencing and piecewise procedures, respectively. In other words, in such a moderate terrain case, the *OC* could be less dependent on the leveling path.

Spectrally, regarding routes (I) and (III), the above two inconveniences may be regarded to an eventual nature of *OC* that could have occasionally varying frequency, dependent on the relevant terrain variability, as implied by Table (3). Accordingly, it could be claimed that an appropriately selected procedure (Eq. 8, 9 or 10), based on the encountered terrain roughness, would furnish relatively accurate values for the *OCs* over leveling lines. In this sense, it could be supposed that the proposed algorithm for *OCs* computation would be self-sufficient and require no further multi-spectral treatment.

From Table 5, one could notice that the *OCs* for elevations could assign very significant values. Such values must be taken into account for ordinary engineering projects in such regions. Also, it is clear that for the investigated elevation ranges, the non-harmonic contribution to the *OCs* is negligible. Moreover, the two harmonic models (with different resolutions) yielded almost the same *OC* features over this very rugged topography.

Finally, the three investigated geopotential models yielded practically the same results. So, it seems that in terms of geoptential coefficients, the *OC* computed by the proposed algorithm might demand a set of harmonic coefficients with low resolution. It could still be lower than the resolution of the two satellite-only models.

7. Recommendations

Based on the obtained results, it is recommended to apply the proposed algorithm for *OC* computation in precise leveling networks. Such proposed algorithm is applicable to any other geographical regions, where the geodetic coordinates of the encountered benchmarks are expressed on the WGS-84 ellipsoid

According to the encountered terrain roughness, the appropriate algorithm procedure might be used. A further work could investigate the maximal degree, beyond which the so computed *OCs* do not gain any additional change. Again, this may be conditioned by the topographic roughness.

On the other hand, trigonometric leveling is the preferred terrestrial leveling technique over rugged topography. In spite of its relatively modest accuracy, the relevant *OCs* over extremely long distances could assign significant values. In such a case, the application of *OC* would not be a matter of spirit leveling only. So, Eq. (9) may be applied to compute

the eventually significant *OCs* for trigonometrically leveled height differences.

Acknowledgements

Three unknown reviewers are acknowledged for their critical review of the manuscript.

References

Abdel-Gawad, A.K., M.E. El-Tokhey and A.M. Abdel-Wahab (2010). Accuracy assessment of SRTM data case study: New Cairo, Hurghada and Toshka in Egypt. Australian Journal of Basic and Applied Sciences, 12(4), 6269-6275.

Bagherbandi, M. and R. Tenzer (2013). Geoid-to-Quasigeoid separation computed using the GRACE/GOCE global geopotential model GOCO02S - A case study of Himalayas and Tibet. Terr. Atmos. Ocean. Sci, 24(1), 59-68.

Burša, M. (1971). Single-layer density as function of Stokes' constants. Studia geoph. et geod.,15, 113-123.

Burša, M. (1975). The scale factor for lengths and the dimension of the Earth's ellipsoid based on the GEM5 and GEM6 systems. Studia geoph. et geod., 19, 291-295.

Ellmann, A., P. Vanček, M. Santos and R. Kingdon (2007). Interrelation between the geoid and orthometric heights, Proceedings. 1st International Symposium of the International Gravity Field Service: Gravity Field of the Earth, Istanbul, Turkey, 28 August - 1 September, 2006, 130-135.

Filmer, M. S., W. E. Featherstone and M. Kuhn (2010). The effect of EGM2008-based normal, normal-orthometric and Helmert orthometric height systems on the Australian leveling network. Journal of Geodesy 84(8), 501-513.

Forsberg, R. and C.C. Tscherning (2008). An overview manual for the GRAVSOFT geodetic gravity field modelling programs, 2. edition, National Space Institute (DTU-Space), Denmark, August.

Hashemi Farahani, H., P. Ditmar, R. Klees , X. Liu, Q. Zhao and J. Guo (2012). The Earth's static gravity field model DGM-1S from an optimal combination of GRACE and GOCE data: Computation and validation aspects. Journal of Geodesy, in review.

Hassouna, R. (2013). Geopotential models as a tool of densifying gravity for orthometric correction computation. Engineering Research Journal, Faculty of Engineering in Shebin El-Kom, Minoufiya University, Egypt, 36(4), 475-479.

Heiskanen, W.A. and H. Moritz (1967). Physical geodesy. W.H. Freeman and Company.

Hwang, C. and Y.-S. Hsiao (2003). Orthometric corrections from leveling, gravity, density and elevation data: A case study in Taiwan. Journal of Geodesy, 77(5-6), 279-291.

Kotsakis, C., K. Katsambalos and D. Ampatzidis (2012). Estimation of the zero-height geopotential level W_0^{LVD} in a local vertical datum from inversion of co-located GPS, leveling and geoid heights: A case study in the Hellenic islands. Journal of Geodesy, 86(6), 423-439.

Manoussakis, G., D. Delikaraoglou and G. Ferentinos (2009). An alternative approach for the determination of orthometric heights using a circular-arc approximation for the plumbline. Proceedings of the 2007 IAG General Assembly: Observing our changing earth, Perugia, Italy, July 2-13, 2007, 245-252.

Mayer-Gürr, T., D. Rieser, E. Höck, J.M. Brockmann, W.D. Schuh, I. Krasbutter, J. Kusche, A. Maier, S. Krauss, W. Hausleitner, O. Baur, A. Jäggi, U. Meyer, L. Prange, R. Pail, T. Fecher and Th. Gruber (2012). The new combined satellite only model GOCO03S**.** Abstract presented at the International Symposium on Gravity, Geoid and Height Systems GGHS 2012, Venice, October 9-12, 2012.

Moritz, H. (1980). Geodetic reference system 1980. Bulletin Géodésique, 54(3), 395-405.

Pavlis, N.K., S.A. Holmes, S.C. Kenyon and J.K. Factor. (2008). An Earth gravitational model to degree 2160: EGM2008. Presented at the 2008 General Assembly of the European Geosciences Union, Vienna, Austria, April 13-18, 2008.

Santos, M., P. Vanicek, W.E. Featherstone, R. Kingdon, A. Ellmann, M. Kuhn, B-A Martin and R. Tenzer (2006). Relation between rigorous and Helmert's definitions of orthometric heights. Journal of Geodesy, 80(12), 691-704.

Tapley, B., J. Ries, S. Bettadpur., D. Chambers., M. Cheng, F. Condi and S. Poole (2007). The GGM03 mean Earth gravity model from GRACE. *Eos Trans. AGU, 88(52), Fall Meet. Suppl., Abstract G42A-03, 2007.*

Tenzer, R., P. Vaníček, M. Santos, W.E. Featherstone and M. Kuhn (2005). The rigorous determination of orthometric heights, Journal of Geodesy, 79(13), 82-92.

USGS (2006). SRTM3, available at: http://dds.cr.usgs.gov/srtm/, (Accessed 5 January 2013).